TARMAKDER
TARIM MAKİNALARI DERNEĞİ

Tarım Makinaları Bilimi Dergisi
Journal of Agricultural Machinery Science

http://dergipark.org.tr/tr/pub/tarmak

Research Article / Araştırma Makalesi

e-ISSN: 2651-4230

20(1), 2024: 1-14

Telescopic Boom Design for Field Sprayers

Tarla Pülverizatörleri İçin Teleskopik Bum Tasarımı

Hasan Berk Özyurt[1,*], İlker Hüseyin Çelen[1]

[1]*Tekirdağ Namık Kemal Üniversitesi, Ziraat Fakültesi, Biyosistem Mühendisliği Bölümü, Tekirdağ, Türkiye.*
** Corresponding author (Sorumlu Yazar): H.B. Özyurt, e-mail (e-posta): berkozyurt@nku.edu.tr*

Article Info

Received date : 28.12.2023
Revised date : 07.04.2024
Accepted date : 24.04.2024

Keywords:

Sprayer boom
Field sprayer
Telescopic motion
3-D modelling
Finite element analysis

Özyurt, H.B., Çelen, İ.H., (2024). *"Telescopic Boom Design for Field Sprayers", Journal of Agricultural Machinery Science, 20(1): 1-14.*

ABSTRACT

The efficiency of pesticide applications has become an important issue with the increasing amount of pesticide usage in agriculture around the world. One of the most vital components of pesticide applications is the sprayer. Sprayers are used to spray the pesticides over the target organism homogenously. The sprayer boom is a crucial component of field sprayers in terms of spray homogeneity. To eliminate the yawn and roll moments on the sprayer booms, the design of those components is crucial. For that reason, a telescopically foldable sprayer boom consisting of 5 parts that hold 24 flat fan nozzles was designed. The materials used in the boom design were St-37 square welded and St-52 bent sheet steels. The relative motion of the boom parts was provided by the wheels that were beared on radial ball bearings. The propulsion was created with the rack-pinion mechanism and a DC motor. In order to examine the strength of the design, statical structural analysis was carried out in the Solidworks simulation module by using the Finite Element Method (FEM). All boom parts, wheels, and boom-chassis support points are investigated individually. All forces affected on the boom parts on both the XY and YZ planes were calculated with the help of the free-body diagrams. Support points, gravity, and external forces were applied before the analysis is carried out. Then, meshes were created. After the mesh creation, the analysis was carried out and Von-Mises stress and displacement graphs were created. According to the graphical results, critical zones on the boom parts were identified and design improvements were performed when necessary.

Makale Bilgisi

Alınış tarihi : 28.12.2023
Düzeltilme tarihi : 07.04.2024
Kabul tarihi : 24.04.2024

Anahtar Kelimeler:

Pülverizatör bumu
Tarla pülverizatörü
Teleskopik hareket
3-D modelleme
Sonlu elemanlar analizi

Atıf için:

Özyurt, H.B., Çelen, İ.H., (2024). "Tarla Pülverizatörleri İçin Teleskopik Bum Tasarımı", Tarım Makinaları Bilimi Dergisi, 20(1): 1-14

ÖZET

Dünya genelinde tarımda pestisit kullanımının artmasıyla birlikte pestisit uygulamalarının verimliliği de önemli bir konu haline gelmiştir. Pestisit uygulamalarının en hayati bileşenlerinden biri pülverizatördür. Püskürtme bumu, püskürtme homojenliği açısından tarla pülverizatörlerinin önemli bir bileşenidir. Pülverizatör bumlarındaki esneme ve yuvarlanma momentlerini ortadan kaldırmak için bu bileşenlerin tasarımı çok önemlidir. Bu nedenle, teleskopik olarak katlanabilen, 24 yelpaze hüzmeli püskürtme memesini taşıyan 5 parçadan oluşan bir pülverizatör bumu tasarlanmıştır. Bum tasarımında kullanılan malzemeler St-37 kare profil ve St-52 bükümlü sac levhadır. Bum parçalarının doğrusal hareketleri radyal bilyalı rulmanlar ile yataklanmış tekerlekler ile sağlanmaktadır. Tahrik, kremayer-pinyon mekanizması ve bir DC motor ile mümkün kılınmıştır. Tasarımın mukavemetini incelemek için Solidworks Simulation modülünde Sonlu Elemanlar Yöntemi (FEM) kullanılarak statik yapısal analizler gerçekleştirilmiştir. Tüm bum parçaları, tekerlekler ve bum-şasi destek noktaları ayrı ayrı incelenmiştir. Bum parçalarına hem X-Y hem de Y-Z düzlemlerinde etki eden tüm kuvvetler serbest cisim diyagramları yardımıyla hesaplanmıştır. Analiz yapılmadan önce destek noktaları, yerçekimi ve dış kuvvetler uygulanmıştır. Daha sonra meshler oluşturup analizler yürütülerek Von-Mises gerilme ve yer değiştirme grafikleri oluşturulmuştur. Grafik sonuçlarına göre, bum parçaları üzerindeki kritik bölgeler belirlenmiş ve gerektiğinde tasarım iyileştirmesi yapılmıştır.

1. INTRODUCTION

Pesticide applications are vital in agriculture and rank among the foremost inputs following mechanization (Demir and Çelen, 2006). Globally, approximately 3 million liters of pesticides are utilized, with Türkiye accounting for about 53,098 liters as of 2020 (Şık and Oyman, 2021). Among the machinery used for plant protection in agriculture, tractor-mounted field sprayers stand as the most preferred type (Bayat and İtmeç, 2018). Türkiye currently registers 365,171 PTO-triggered field sprayers officially (TUIK, 2019).

These sprayers employ a system referred to as a 'spray bar,' 'sprayer booms,' or simply 'boom,' consisting of various foldable parts designed for transport convenience. Hydraulic actuators or manual means are utilized to fold the middle and outer parts over the central boom frame for transport purposes. Typically, these boom parts are constructed from square welded steel materials, which are cut and welded together to form the boom structure (Fig. 1).

Figure 1. Example of field sprayer booms (Badilli Agricultural Machinery)

The design and operational dynamics of the boom play a pivotal role in achieving spray uniformity and preventing drift. Variations in the horizontal and vertical positions of the boom during spraying, caused by vibrations due to uneven field terrain or contact of the tractor/sprayer with the ground, significantly impact spray consistency (Ooms et al., 2003). During operation, the sprayer boom undergoes roll and yaw moments along two axes, a well-documented occurrence in relevant literature (Fig. 2). The influence of momentary forces on the horizontal axis can abruptly nullify the relative speed between the sprayer's boom and the ground, potentially resulting in increased pesticide dosage on specific treated areas (Matthews, 2008).

(a) (b)

Figure 2. (a) Roll moment, (b) Yaw moment (Bjornsonn et al., 2013)

A prevailing issue with sprayers in Türkiye stems from the small and irregularly shaped fields. Operators have to readjust the sprayer boom when entering a field and then return it to the transport position when the field work is completed, which requires frequent dismounting from the tractor. This process is time-consuming. While the development of hydraulically foldable booms has alleviated this issue, the preference for these booms among farmers is hindered by the costliness of hydraulic actuators and hoses, which also add excess weight to the sprayer (Özyurt et al., 2020).

Moreover, spray applications typically follow tramlines. In uneven or irregular areas, starting spraying from a straight edge may result in unfinished tramlines or untargeted areas narrower than the sprayer's working width. Additionally, certain field areas may contain obstacles like electrical poles, telephone or natural gas pipeline markers, old wells, irrigation pump sites, trees, and bushes. These obstacles could lead to overlapping spray or unintentional application on non-targets if all nozzles remain open. In cases where pesticide rates are finely calibrated, an overdose might harm primary plants or beneficial organisms within the field.

Research on field sprayer booms focuses on analyzing their behavior under dynamic conditions, strain assessment in both dynamic and static settings, understanding the impact of design on spray distribution, and exploring folding mechanisms. Fujita and Sugiyama (2012) conducted dynamic analyses of sliding supports in telescopic cranes using the absolute node coordinate formulation, highlighting that stress points and axes shift as the crane's length changes over time. Similarly, Raftoyiannis and Michaltsos (2013) studied the dynamic behavior of telescopic crane arms, developing a model for their dynamic analysis. Their findings revealed minimal dynamic deformations in the moving part during folding, substantially higher deformations during folding compared to the resting state, and reduced deformations at higher folding speeds. In parallel, studies by Lupea et al. (2009) and Manea et al. (2018) simulated the boom structure of field sprayers under dynamic conditions. Utilizing 3D models and finite element analysis software, they examined boom behavior statically and dynamically, optimizing its structure. Their simulations indicated vibrations at the boom tip with small wavelengths, causing significant displacements. However, they found no risk of material failure or deformation, as the Von Mises maximum equivalent stress remained below the yield strength of the boom parts. Additionally, Zhang et al. (2019) determined natural frequency values under dynamic conditions, identifying these as critical design parameters for future boom designs.

In this study, it is aimed to design a linear moving boom system with an alternative design and folding mechanism to conventional booms, which can meet the application efficacy criteria and expectations of farmers. In addition, static structural analyses were performed to achieve the most resilient and lightweight design.

2. MATERIALS AND METHODS

In this study, a solution-oriented design for the boom section of a traditional field sprayer was developed, addressing prevalent issues. The newly designed boom replaces the original one on a sprayer featuring a chassis constructed by 60x60 mm welded squares and equipped with a 1000-liter polyethylene tank. The original boom, consisting of 40x40 and 80x40 welded squares, is manually folded into five parts along the horizontal axis. It supports 24 spray nozzles at 50 cm intervals, providing a total working width of 12 meters for the sprayer. A diaphragm pump with a maximum pressure of 50 bar and a flow rate of 200 l min^{-1} is attached to the sprayer.

Commonly, modern sprayer manufacturers opt for steel materials due to their availability, cost-effectiveness, and ease of processing (Khalifeh et al., 2018). For systems like sprayer booms, which experience high effective moments at distant endpoints from support, additional materials and a robust frame design are necessary to ensure durability. Although St37 (SJ235), the prevalent structural steel in agricultural machinery, has been the preferred choice, there has been a recent shift towards St52 (SJ355) due to its higher tensile strength, better machinability, and reduced cost, making it more affordable. These two materials differ in their elemental compositions, resulting in distinct mechanical properties as outlined in Table 1.

Table 1. Mechanical properties of St37 and St52 steels (Seitl et al., 2020)

Properties	***St37 (S235)***	***St52 (S355)***
Young Modulus (GPa)	208.2±4.1	205.4 ±7.4
Yield Strength (MPa)	276.87±0.31	381.94±6.22
Tensile Strength (MPa)	423.86±1.49	554.41±1.62
Elongation at break (%)	21.99±0.22	34.22 ±1.54
Poisson ratio (-)	0.3	0.3

2.1. Materials Used in the Design

The designed sprayer boom utilizes St37 profiles and St52 steel sheet material as its primary structural components. Comprising four outer boom parts—two on each side—and a central chassis carrying these parts, the boom transitions between transport and field positions. During transport, the outer boom parts fold onto the central chassis, while in the field position, they extend telescopically to the sides. Facilitating telescopic movement, a gear driven by a position-controlled servoelectric motor propels the rack gear, enabling linear movement of the boom part. A linear rail system, propelled by a specially shaped ball bearing wheel, supports and guides this linear movement, ensuring a controlled motion between the boom's parts. Each side of the boom hosts five nozzles, while the central chassis holds six.

2.2. Method

The primary design criterion for the sprayer boom was to achieve 12 meters working width, aligning with the preferred width in the Thrace region and accommodating 24 flat fan nozzles at 50 cm intervals. St52 material, valued for its ductility, ease of bending, and high yield strength, was chosen for the bent sheet metal used in the design. The Solidworks software facilitated the assembly of all boom parts and fasteners. A telescopic design was incorporated, integrating linear rail and wheel configurations to minimize friction between boom parts during movement. Careful selection of wheels and bearings was based on radial load considerations, fatigue strength due to the boom's opening and closing frequency, and material durability. Following the preliminary design, thorough static analysis using Solidworks' Simulation module pinpointed critical stress areas in separate boom parts. Reinforcement and design modifications were strategically implemented in these stress-exposed regions. Material removal from non-stressed areas aimed to optimize the design, resulting in a robust yet lightweight configuration based on the structural analyses conducted.

2.2.1. Telescopic Folding Mechanism

The folding mechanism of the boom operates on a telescopic structure that moves in a linear fashion, employing machine components specifically crafted for linear motion. Electric motors situated close to

the central frame drive this linear motion through a combination of spur gears and rack gears. This setup facilitates relative movements among the boom sections, enabling smooth transitions between transport and operational positions. To achieve this functionality, four servo electric motors, each responsible for controlling a distinct part of the boom, are employed. These motors are adaptable for both manual and automatic control from the driver's cabin. They were chosen for their compatibility with a 12V (5.2A) battery voltage, a rotational speed of 60 rpm, and a cost-effectiveness akin to the wiper motors found in cars. The rack gears, with specifications of n=3 module and a width of 20 mm, cover distances of 2800 mm on the central boom section and 2400 mm on the middle boom part. They are designed to stop just before reaching the last tooth, ensuring precise control over the working width. Additionally, a linear rail system has been integrated into the central frame and middle boom part using shaped sheets, facilitating smooth linear movement and extending the lifespan of the motors. This system incorporates four wheels, two positioned at the top and two at the bottom, which glide along these rails, allowing the boom sections to move over each other seamlessly, similar to a drawer.

Moreover, to prevent deformation when the boom tips encounter obstacles or the ground, the outer boom parts are constructed in two segments with a torsion spring mechanism between them (Fig. 3). This design enables the outer boom parts to elongate upon contact with external forces, safeguarding other components of the boom mechanism from potential damage.

Figure 3. Torsion spring

Solidworks software (Dassault Systems, 2018) served as the primary tool for designing, modifying, and translating technical drawings for machine operators. Structural analyses, aiming for maximum strength with minimal material usage, were conducted using Solidworks' simulation module. Firsty the support points were determined, then the weight and external forces were defined. Von-Mises stresses (Manea et al, 2018; Han et al., 2013) and displacement graphs were generated when the analyses were carried out after the mesh creation process in Solidworks Simulation Module. According to the results of the analyses, the regions with critical stresses were determined and design improvements were made where necessary.

2.2.2. Load Calculations

The telescopic boom system faces two primary critical loadings: the weight of the boom parts and the vertical accelerations encountered on rough terrain during field operations. Our study focused on the statical load, which is gravity and all structural analysis is carried out on static forces. The static load exert forces in both the X-Y and Y-Z planes, necessitating a free-body diagram to determine their direction and magnitude. The analysis focuses on the working position, where the boom system

experiences maximum stress. Mass distances from support points in the X-Y plane and wheel placements are illustrated in Figure 4. Additionally, Figure 5 displays the outer boom, middle boom, and main frame, respectively. Lastly, all the force and distance values are given in Table 2. Due to the symmetrical nature of the right and left boom groups in the Y-Z plane, calculations performed for one direction in the force analysis apply equally to the other side.

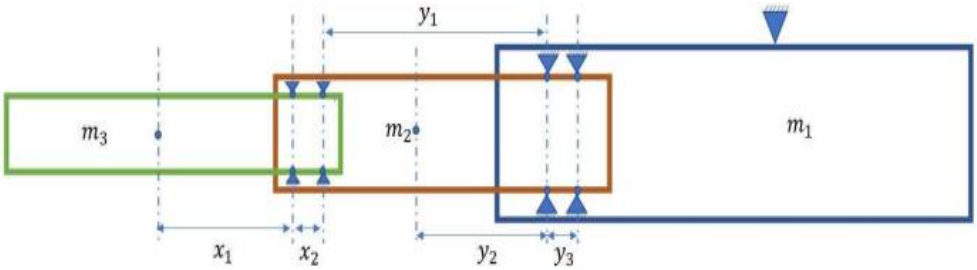

Figure 4. The distance of the centre of gravity of the boom part from the support points on the X-Y plane

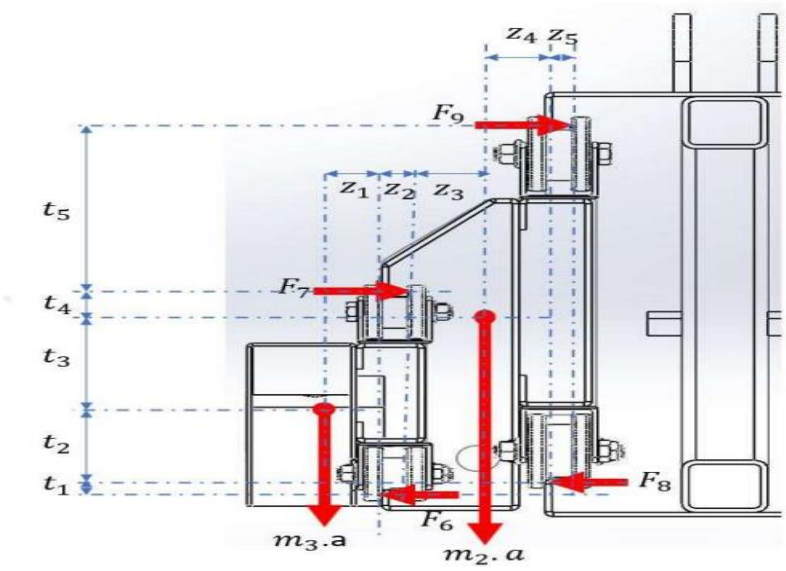

Figure 5. Distance of the centre of gravity of the boom part from the support points and forces on the Y-Z plane

Table 2. Force and distance values

Symbol	*Unit*	*Value*	*Symbol*	*Unit*	*Value*
X₁	mm	895.46	Z_5	mm	15
X₂	mm	130	T_1	mm	12
y₁	mm	2072.5	T_2	mm	56.89
Y₂	mm	973.5	T_3	mm	81.55
Y₃	mm	165	T_4	mm	36.06
Z₁	mm	27.62	T_5	mm	162
Z₂	mm	15	M_1	kg	20
Z₃	mm	57.76	M_2	kg	58
Z₄	mm	22.74	M_3	kg	95

3. RESULTS AND DISCUSSION

The main frame, situated centrally within the boom mechanism, remains fixed during both transport and operational phases. Its design combines welded square and bent sheet metal elements. Welded squares serve as support for carrying the middle and outer boom parts, forming a foundational framework for the entire boom structure. Horizontal 50x50x4 mm welded squares, evenly spaced in the vertical direction, support the top and bottom sections. Meanwhile, 4 mm-thick bent sheet metal, welded to these profiles, reinforces the framework, preventing bending during operational and transport loads. Sheet metal plates on the right and left sides further fortify this structure. Moving to the middle boom, it achieves field position through linear movement along the main frame, while the third element carries the outer boom. The middle boom, composed of spot-welded 4 mm sheet metal sheets shaped in a 'C,' integrates wheels along its inner side for linear movement. Laser cutting removes low-stress sections, reducing overall boom weight. Wheels, placed at 165 mm intervals on the upper and lower surfaces, balance forces from the outer boom's weight. Two M12 bolts fasten each wheel. The outer boom, positioned at the boom's end, also moves linearly on the middle boom. It comprises spot-welded 3 mm sheet metal sheets, shaped similarly in a 'C,' reducing load on the middle boom and minimizing extra weight. Wheels on the inner side facilitate linear movement, placed at 130 mm intervals on the upper and lower surfaces after laser cutting removes low-stress areas (Fig. 6).

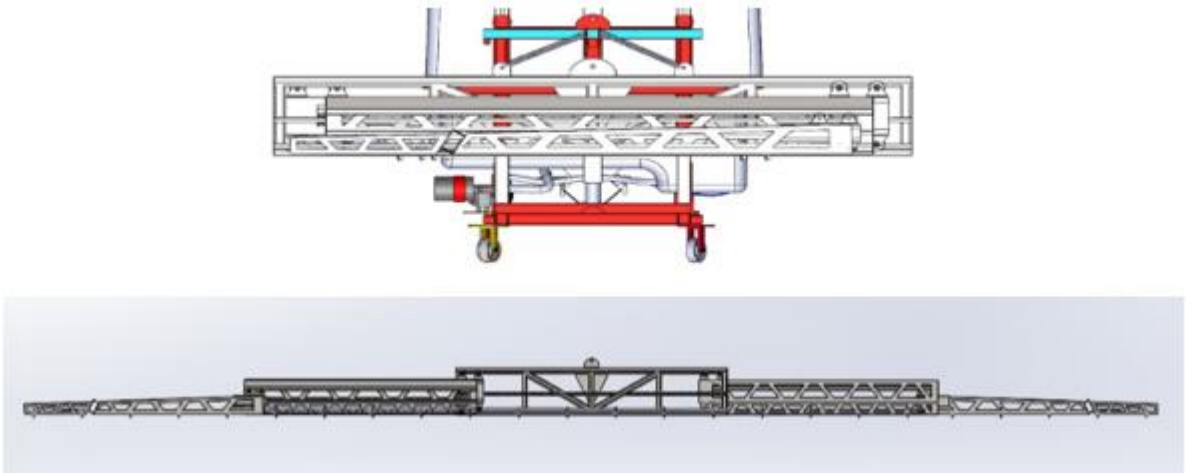

Figure 6. 3D Modelling of the boom

3.1. Von-Misses Stress Analysis of the Outer Boom Part

The structural analysis focused on the outer boom part, employing a finite element method with 12,912 elements and 28,404 nodal points, as depicted in Figure 7. Green arrow indicators denote fixed support locations, while the red arrow represents the center of gravity exerting a force of 196.2 N on the boom. This analysis aims to assess stress distribution and structural behavior within the outer boom section.

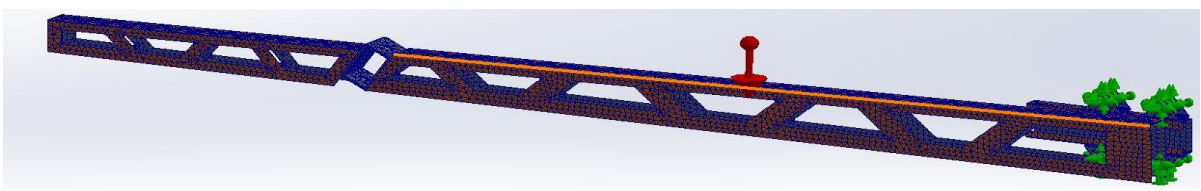

Figure 7. Meshes on the outer boom part

During the simulation, Von-Mises stresses, depicted in Figure 8, were observed after establishing supports, force, and mesh configurations. The color-coded diagram illustrates stress levels across the structure. Predominantly, minimal stresses were evident throughout the boom, with a maximum stress of 48 MPa identified. Notably, this value is 7.9 times lower than the yield strength of St52 Steel, which stands at 381 MPa (Seitl et al., 2020). This calculation indicates a safety factor of 7.9 for the outer boom part.

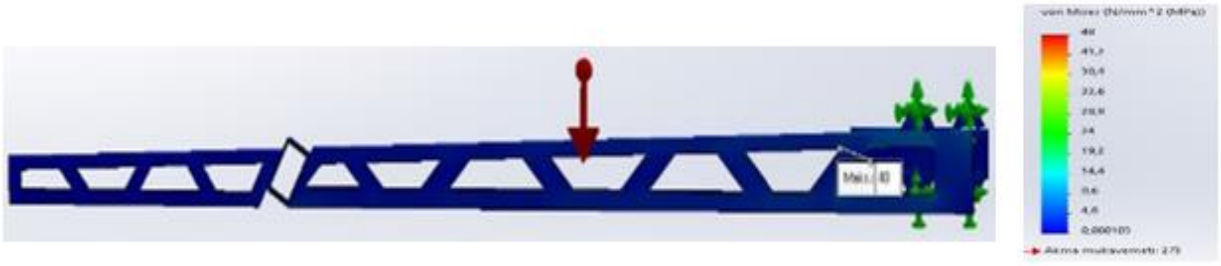

Figure 8. Von Misses Stress Analysis of the outer Boom Part

The bending stress experienced on the outer boom caused slight deformation of the sheet metal, as shown by displacement graphs in the analyses (Fig. 9). These displacements show increasing vertical deviations from the support points toward the boom tip. The maximum measured displacement was 2.21 mm. Considering that the distance between the spraying nozzle tip and the top leaves of the plant is 500 mm, this deformation appears negligible and does not pose a risk to spraying uniformity.

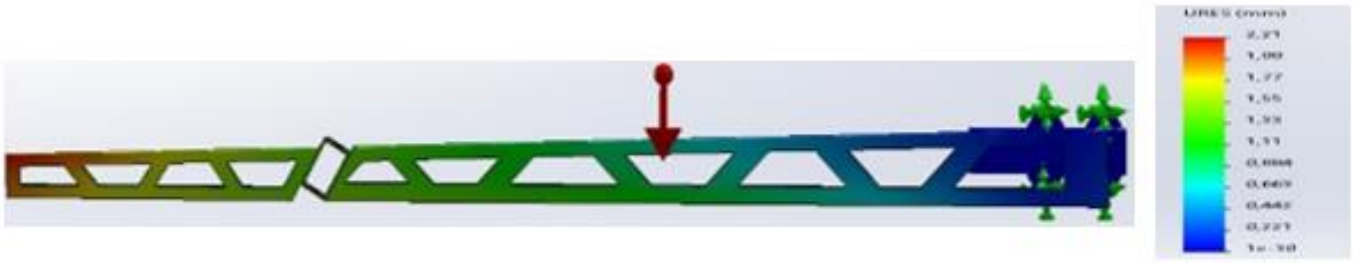

Figure 9. Displacement Analysis in the outer boom part

3.2. Von-Misses Stress Analysis of the Inner Boom Part

In the examination of the middle boom part, the boom was affixed to the wheel hub, considering boom weight as an external load, and applying forces acting on the outer boom part's wheels to contact points on the inner boom. Mesh creation resulted in 13,119 finite elements and 29,028 nodal points on the outer boom part. Figure 10 displays the mesh configuration, support points, and external loads for this analysis.

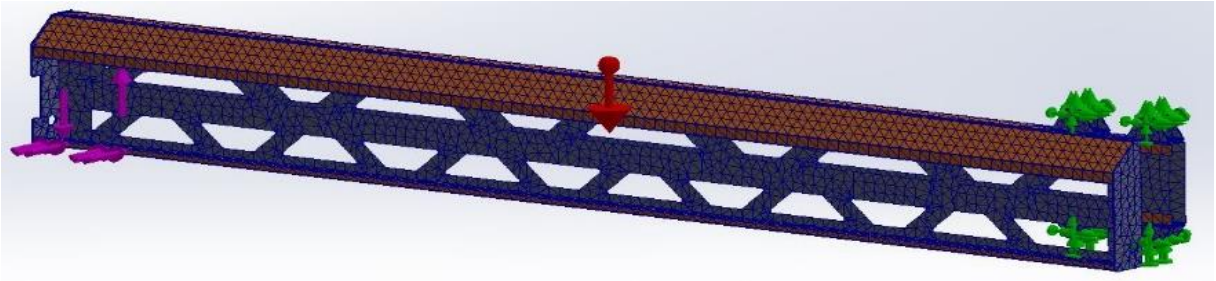

Figure 10. Meshes, support points, and external forces on the middle boom part

In the analysis following the establishment of support points, forces, and mesh, Von-Mises stresses were represented in the graph (Fig. 11). Although predominantly low stresses were observed across the outer boom part, the maximum stress measured was 148 MPa. This value stands at 2.57 times lower than the yield strength of St52 steel, specified at 381 MPa (Seitl et al., 2020). Consequently, the safety factor calculated for the outer boom part is 2.57.

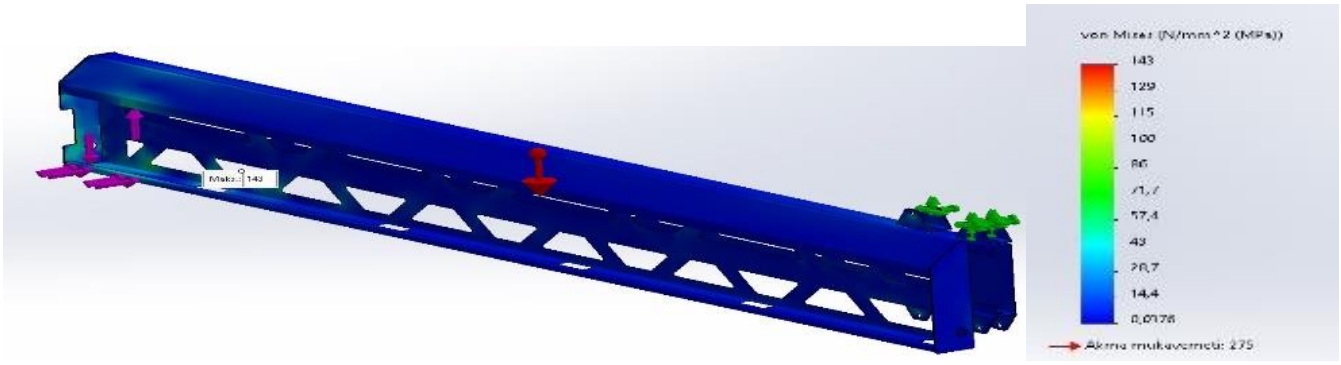

Figure 11. Von Misses Stress Analysis of the middle boom part

The bending stress experienced on the middle boom part caused deformation of the sheet metal, evident in the displacement graph (Fig. 12). These vertical displacements progressively increase from the support points toward the boom tip. The maximum measured displacement was 1.6 mm on the sheets where the outer boom part's wheels rest. Considering this value and its minimal impact on the outer boom's linearity, along with a nozzle tip-to-plant-top distance of 500 mm in spraying applications, this displacement remains inconsequential and poses no risk to spraying uniformity.

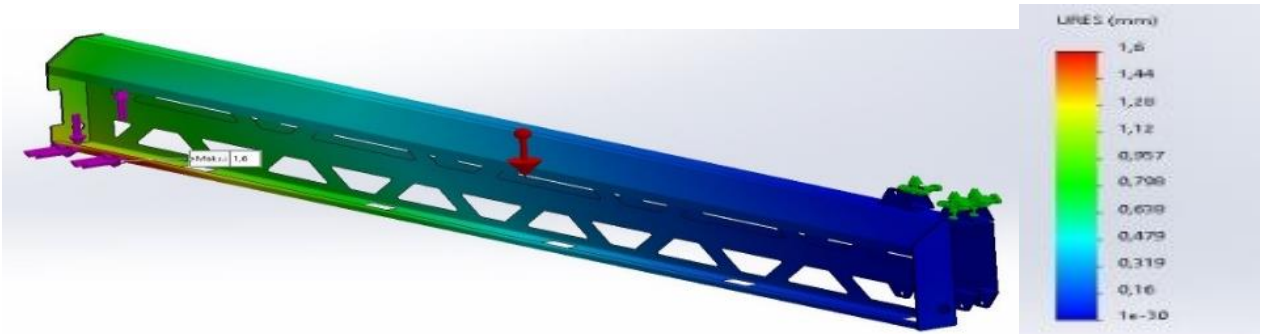

Figure 12. Displacement Analysis in the outer boom part

3.3. Von-Misses Stress Analysis of the Main Frame

During the examination of the primary boom frame, it was affixed to the sprayer chassis at specified connection spots. External forces considered comprised the frame's weight and forces derived from the middle boom parts, applied following free body diagrams. As a result, meshing generated 43,371 finite elements and 87,375 nodal points across the main frame. Figure 13 depicts the mesh layout, support junctures, and the weight load considered within this analysis.

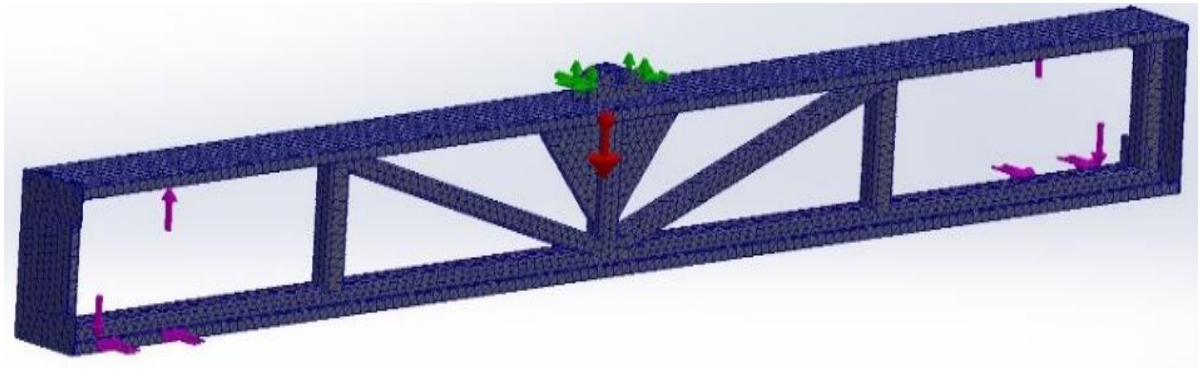

Figure 13. Meshes, support points, and external forces on the middle boom part

In Figure 13, components denoted by green arrows are designated as fixed supports in the simulation. The red arrow signifies the boom's weight, measured at 931.95 N, while the pink arrows represent the forces exerted on the middle boom part. Following the establishment of support points, forces, and mesh, Von-Mises stresses are depicted in the graph (Fig. 14).

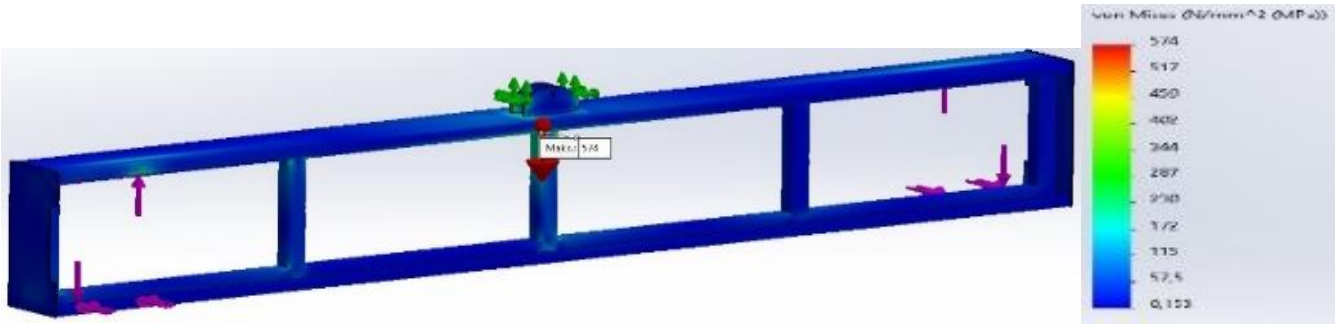

Figure 14. Von Mises Stress Analysis of the main frame

In Figure 14, the simulation revealed significantly high stresses resulting from the forces acting on the middle boom part, with a maximum stress calculated at 574 MPa. This tension, observed in the St-37 profile, exceeds twice the yield strength of 276 MPa. Consequently, the current design of the main frame is deemed structurally inadequate and susceptible to breakage in production. To address this issue, initial design enhancements were proposed. One suggestion involves welding a 15 mm thick bar on both sides of the upper horizontal profile and the junction of the middle vertical profile in the main frame. Upon re-running the analysis with these modifications, stress distributions shown in Figure 15 are observed.

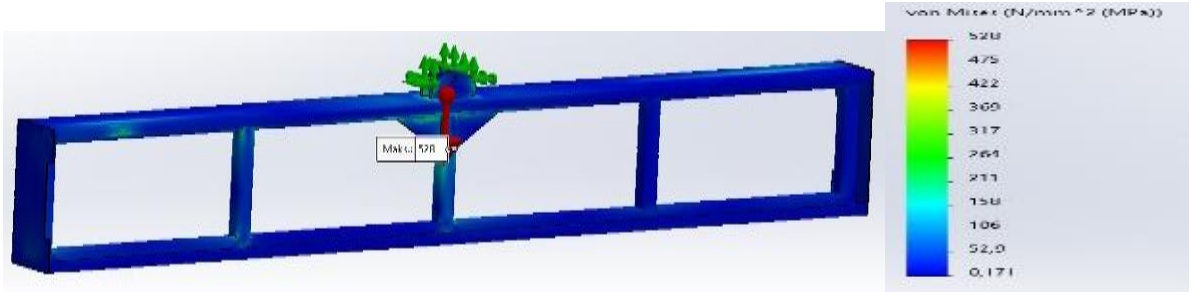

Figure 15. Von Misses Stress Analysis of the main frame after two support plates added

Figure 15 indicates a reduction in the maximum stress value (529 MPa); however, the area with the highest stress persisted above the triangular bar, surpassing the yield strength. As a second design alteration, two support profiles were introduced diagonally from the upper horizontal profile to the lower horizontal profile to augment the inter-profile support. Moreover, enhancing the triangular support plate's vertical dimensions aimed to diffuse stress concentration. Upon re-running the analysis following these enhancements, the resulting stress distribution is depicted in Figure 16.

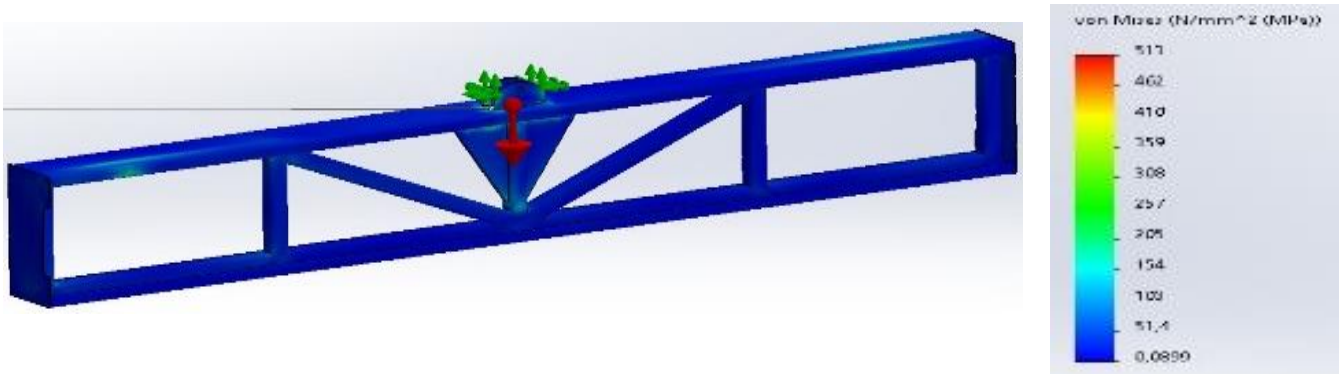

Figure 16. Von-Mises Stress Analysis of the main frame after two bigger support plates and support profiles added

In the depicted graph, following the implemented enhancements, the highest stress point, reaching 513 MPa, was identified at a support point external to the frame. Figure 17 illustrates the maximum stress experienced by the frame itself.

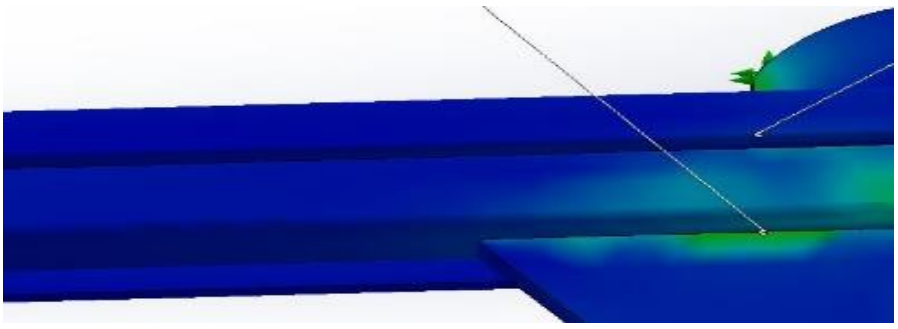

Figure 17. Maximum stress area on the main frame

The graph illustrates that the recent enhancements resulted in a peak stress of 277 MPa within the support frames. These frames, constructed from St52 material boasting a yield strength of 381 MPa, now exhibit stress levels below the yield strength threshold. Additionally, the displacement graph resulting from the analysis, displaying the integration of cross-support profiles as shown in Figure 18, aligns closely with the expected outcomes.

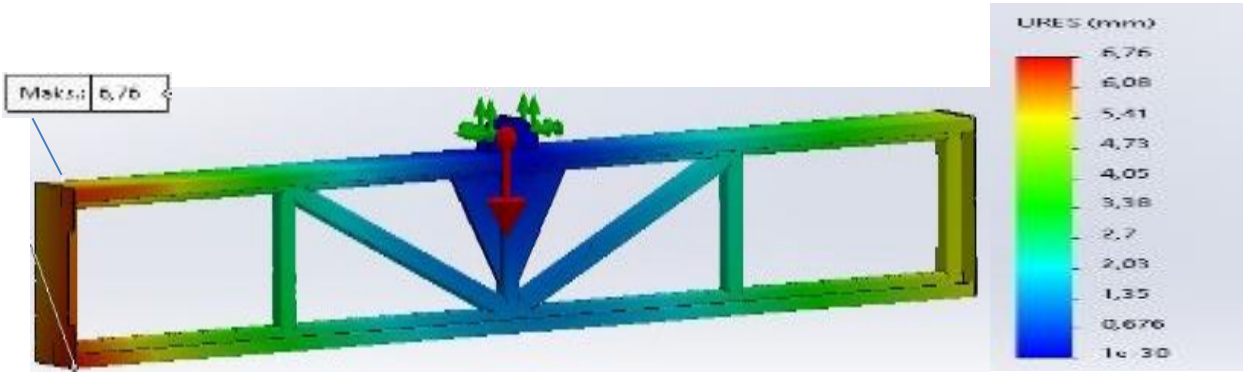

Figure 18. Displacement Analysis on the main frame

A displacement of 6.7 mm is within acceptable parameters for this design. However, further enhancements can be considered once all the boom parts are assembled during the production phase, specifically targeting improvements in the main frame.

4. CONCLUSION

The study introduces a telescopic foldable boom design tailored for field sprayers used in crop protection. This system comprises five parts, boasting 12 meters working width and 24 fan spray nozzles spaced at 50 cm intervals. The design allows for transport without surpassing the allowable working width on public roads. Among these five parts, one serves as the central support for the remaining four, organized in pairs on the right and left, capable of relative linear movement for transitioning between operational and transport configurations. This telescopic folding boom system spans 11,702 mm in the operational position and 2,800 mm while on the road, with a total mass of 275 kg. Despite a comparable mass, this design showcases enhanced structural safety and stability compared to conventional sprayer booms. Utilizing Solidworks' simulation module, static structural analyses were conducted employing finite element methodology. The assessment involved determining forces acting on the boom and support points through free-body diagrams, followed by integrating these forces into the analysis. The analyses affirmed the safety of the outer and middle boom parts, whereas the initial design of the central mainframe raised safety concerns. Subsequent enhancements, incorporating additional profiles and support plates, resulted in a structurally sound boom. This innovative boom system offers several advantages over conventional spraying equipment. Symmetrical opening and closing between transport and working positions prevent shifts in the boom's center of gravity. Moreover, electronic control from the tractor cabin allows the boom part facing potential collisions with obstacles like poles or trees to move closer to the transport position, averting collisions. In contrast, conventional sprayers require the tractor to maneuver around obstacles. Lastly, internal placement of the spray nozzles within the boom frame shields them from external impacts.

REFERENCES

Badilli Agricultural Machinery (2021, Mayıs 2021). *Transport and working position of a field sprayer.* Badilli Company. https://www.badilli.com.tr/tr/urunler-2/cobra_600_tarla_ilaclama-69.html (erişim tarihi: 04.05.2021)

Bayat, A., Itmec, M. (2018). The current state of sprayer manufacturers in Turkey and some strategies for the future. *Scientific Papers-series A. Agronomy*, 61(2), 105-108. https://agronomyjournal.usamv.ro/pdf/2018/issue_2/Art18.pdf

Dassault Systèmes SE (2018). Solidworks 2018 Vélizy-Villacoublay, France.

Demir, C., Çelen, İ. H. (2006). Tekirdağ ilindeki tarımsal işletmelerdeki pülverizatörlerin durumu ve sorunları üzerine bir araştırma. *Journal of Agricultural Sciences*, *12*(01). https://dergipark.org.tr/tr/download/article-file/2693511

Fujita, H., Sugiyama, H. (2012). Development of flexible telescopic boom model using absolute nodal coordinate formulation sliding joint constraints with lugre friction. *Theoretical and Applied Mechanics Letters*, 2(6), 063005. https://doi.org/10.1063/2.1206305

Han, H., Chen, S., Shao, J., Yao, Y., and Chen, G. (2013). Lightweight design of chassis frame for motor boom sprayer. *Transactions of the Chinese Society of Agricultural Engineering*, *29*(3), 47-53.

Jeon, H.Y., Womac, A.R., and Gunn, J. (2004). Sprayer boom dynamic effects on application uniformity. *Transactions of the ASAE*, *47*(3), 647-658.

Khalifeh, A. R., Banaraki, A. D., Manesh, H. D., Banaraki, M. D. (2018). Investigating of the tensile mechanical properties of structural steels at high strain rates. *Materials Science and Engineering: A*, 712, 232-239.

Lupea, I., Tudose, L., Stanescu, C. M., Lupea, M. (2009). Dynamic symulation and experimenton a sprayer boom structure. B. Katalinic (Editör), *20th DAAAM International Symposium on Intelligent Manufacturing and Automation*, 1541-1542.

Manea, D., Gidea, M., Marin, E., Mateescu, M. (2018). Simulation of mechanical parameters of sprayer boom. *Engineering for Rural Development,* 17, 45–51. https://doi.org/10.22616/ERDev2018.17.N048

Matthews, G. (2008). *Pesticide application methods* (3. Baskı). John Wiley & Sons.

Ooms, D., Ruter, R., Lebeau, F., and Destain, M. F. (2003). Impact of the horizontal movements of a sprayer boom on the longitudinal spray distribution in field conditions. *Crop protection*, *22*(6), 813-820.

Ozyurt, H. B., Onler, E., and Celen, I. H. (2020). Determination of the field sprayers and their problems in Thrace Region, Turkey. *International Journal of Innovation Engineering and Science Research*, 4(6), 68-73.

Raftoyiannis, I. G., Michaltsos, G. T. (2013). Dynamic behavior of telescopic cranes boom. *International Journal of Structural Stability and Dynamics*, 13(1). https://doi.org/10.1142/S0219455413500107

Seitl, S., Pokorný, P., Miarka, P., Klusák, J., Kala, Z., and Kunz, L. (2020). Comparison of fatigue crack propagation behaviour in two steel grades S235, S355 and a steel from old crane way. *MATEC Web of Conferences (Vol. 310) 2019 (1-6).* K. Kotrasová, E. Kormaníková and S. Kmeť (Editörler). EDP Sciences.

Şık, B., Ayman, O., 2021. *Zehirsiz sofralar*. Sistemik Dijital Kitap Atelyesi, Buğday Ekolojik Yaşamı Destekleme Derneği, AB Projesi, Kitap. www.zehirsizsofralar.org

Turkish Statistical Institute (TUIK), (2019). Number of Field Sprayers. Retriewed from: https://data.tuik.gov.tr/Kategori/GetKategori?p=tarim-111&dil=1

Zhang, J., Wang, X., and Li, S. (2019). Finite element modeling and robust control of plant protection machine boom. *Journal of Advanced Agricultural Technologies*, 6(4), 257–262. https://doi.org/10.18178/joaat.6.4.257-262

Authors' Biography

Hasan Berk ÖZYURT

08.06.1994 yılında Tekirdağ'da doğdu. İlk ve ortaöğrenimini Tekirdağ'ın Muratlı ilçesinde tamamladı. 2012 yılında Tekirdağ Belediyesi Anadolu Öğretmen Lisesi'nden mezun oldu. Aynı yıl İstanbul Teknik Üniversitesi Makine Fakültesi Makine Mühendisliği Bölümünde lisans hayatına başladı. Lisans hayatı boyunca Türk Traktör Ziraat Makineleri A.Ş., Claas, Hema Endüstri A.Ş. firmalarında stajyer mühendis olarak görev yaptı. 2017 yılında İ.T.Ü. Makine Mühendisliği'nden mezun oldu. Aynı yıl Tekirdağ Namık Kemal Üniversitesi Biyosistem Mühendisliği Anabilim Dalı'nda yüksek lisans eğitimine başladı. 2020 yılından beri Tekirdağ Namık Kemal Üniversitesi Ziraat Fakültesi Biyosistem Mühendisliği Bölümü Tarımda Makine Sistemleri Anabilim Dalı'nda Araştırma Görevlisi olarak görev yapmaktadır. Şu ana kadar yayınladığı 4 makale, 2 kitap bölümü, 4 kongre bildirisi bulunmaktadır.

İletişim berkozyurt@nku.edu.tr

ORCID Adresi https://orcid.org/0000-0003-0775-1723

Prof. Dr. İlker Hüseyin ÇELEN

08.03.1971 yılında İstanbul'da doğdu. İlk ve orta öğrenimini Hatay İskenderun ilçesinde tamamladı. 1992 yılında Ankara Üniversitesi Ziraat Fakültesi Tarım Makinaları Bölümünden Ziraat Mühendisi olarak mezun oldu. Aynı Bölümde 1995 yılında Yüksek Lisans Eğitimini tamamladı. 1994 yılında Trakya Üniversitesi Tekirdağ Ziraat Fakültesi Tarım Makinaları Bölümünde Araştırma Görevlisi olarak göreve başladı ve aynı Bölümde 1999 yılında Doktora eğitimini bitirdi. 2000 yılında Yardımcı Doçent olarak Trakya Üniversitesi Tekirdağ Ziraat Fakültesi Tarım Makinaları Bölümüne atandı. 2011 de Namık Kemal Üniversitesi Ziraat Fakültesi Biyosistem Mühendisliği Bölümüne Doçent olarak atandı ve aynı Bölümde 2018 yılında Profösör oldu. Tarım Makinaları ve özellikle Bitki Koruma Makinaları ve otomasyonu konusunda çalışmalar yapan araştırmacı konusunda birçok kongrede bildiri sunmuş, yurt içi ve yurt dışı birçok makalesi yayınlamıştır. Birçok projede görev alarak 3 adet patent sahibi olmuştur. Ayrıca yayınladığı 2 kitap ve bölüm yazarlıkları vardır.

İletişim icelen@nku.edu.tr

ORCID Adresi https://orcid.org/0000-0003-1652-379X